Liu, Deng and Chu (eds) © 2008 Science Press Beijing and Springer-Verlag GmbH Berlin Heidelberg
Geotechnical Engineering for Disaster Mitigation and Rehabilitation

LIQUEFACTION OF SAND UNDER BI-DIRECTIONAL CYCLIC LOADING

Maotian Luan, Dan Jin, Zhendong Zhang and Qiyi Zhang
State Key Laboratory of Coastal and Offshore Engineering, Dalian University of Technology, Dalian 116024, China
Institute of Geotechnical Engineering, School of Civil and Hydraulic Engineering, Dalian University of Technology, Dalian 116024, China

A laboratory study is presented of liquefaction behavior of saturated loose sand subjected to bi-directional cyclic loading under isotropic consolidated conditions using the soil static and dynamic universal triaxial and torsional shear apparatus, which can apply axial pressure W and torque M_T individually. Tests were performed following the stress path that is controlled by shape of ellipse in terms of axial component $\sigma_d/2$ and torsional component τ. In this type of loading pattern the progressive rotation of orientation of principal stress axe and the unequal transverse and longitudinal cyclic components can be realized for simulating the complex stress condition induced by wave or earth embankments. For equivalent ratio of $\sigma_d/2$ to τ, the cyclic loading resistance decreases with the increasing area bounded by the elliptical stress path. And for the same area of the elliptical stress path, the sample exhibits the highest resistance to liquefaction when the ratio of $\sigma_d/2$ to τ reaches a critical value which equals to 0.6~0.75. The deformation behavior of sand is also considerably associated with the proportion of $\sigma_d/2$ to τ.

INTRODUCTION

Until recently, the major concern during earthquake loading of saturated sands was to against the occurrence of liquefaction. Saturated granular materials, such as sands and silts, when is subjected to cyclic loading, the tendency of compact and decrease in volume will occur, and thus will generate excess pore water pressure if the drainage is prevented. The pore water pore pressure reaches the effective stress, what is known as liquefaction occurs.

Many studies have been done concerning with the characteristics of deformation and strength of sands in liquefaction. However, most of them are restricted in the behaviors of sands under narrow loading conditions, and cannot explain the characteristics under complex stress condition such as the cyclic stress induced by wave loading which characterized by the

fact that the orientation of principal stress axe rotates progressively. Cyclic simple tests such as triaxial shear test and torsional shear test are not able to reproduce the above-mentioned complex stress condition and cyclic loading pattern (Fu, 2000). Therefore, the efforts have been made by several researchers to well develop the soil experimental technology.

Seed (1975) has revealed that the multidirectional cyclic resistance is less than one-directional cyclic resistance by multidirectional shaking tests on dry sand. Boulanger (1995) has researched the liquefaction of sand under bi-directional loading and pointed out hat the perpendicular cyclic loading resistance is lower than parallel cyclic loadings. Pyke et al. (1975) also accomplished bi-directional simple shear loading to evaluate the effects of bi-directional shaking on the deformation of dry sands. All the researches show that the rotations of principal stress axe influence the behavior of sand remarkably. Since the valuable laboratory data is extraordinary rare and not comprehensive, especially in the field of bi-directional cyclic loading with unequal peak value separately. This paper is aim to find some useful information about this issue by implementing sets of laboratory tests using the advanced soil static and dynamic universal triaxial and torsional shear apparatus.

The soil static and dynamic universal triaxial and torsional shear apparatus, which was accomplished in the Institute of Geotechnical Engineering, Dalian University of Technology after importing from Seiken Corp., Inc, was used in this paper. The apparatus enables simultaneously exertion and individually control of axial pressure W, torque M_T, outer chamber pressure p_o and inner chamber pressure p_i and combination of these components. Therefore the consolidation and loading paths under different complex stress conditions of soils can be implemented. It constitutes a well-performed universal test system that makes possible to conduct a great deal of experimental tests of soil under various complex stress conditions. Furthermore comprehensive and systematic analyses on deformation and strength characteristics of saturated loose sand under monotonic and cyclic shear loading are carried out.

EXPERIMENTAL TECHNIQUE

Hardware

The soil static and dynamic universal triaxial and torsional shear apparatus used for the experiments is composed of five components including main unit, air-water unit (air compressor and vacuum pump), analogue control unit, data acquisition and automatic control system and hydraulic servo loading unit (hydraulic actuators and hydraulic supply). The details concerning this comprehensive system were given by Luan et al. (2003).

Material and sample preparation

Please preserve the style of the headings, text font and line spacing in order to provide a uniform style for the proceedings volume. The materials used for this experimental study is

the Chinese Fujian Standard Sand. The basic properties were as follows: specific gravity G_s=2.643; granular size d_{50}=0.34mm; uniformity coefficient C_u=1.542; the maximum and minimum void ratios e_{max}=0.774 and e_{min}=0.537; and the maximum and minimum dry unit weights ρ_{max}=1.72g.cm^{-3} and ρ_{min} =1.49g.cm^{-3}.

The sand sample is prepared by pluviation through air. Saturation of the sample is fulfilled by pouring both CO_2 and de-air water and by exerting backpressure. Consolidation and cyclic stress-controlled tests are carried out on the hollow cylinder soil samples with height of 150mm, outer diameter of 100mm and inner diameter of 60mm. All samples are tested undrained with pore pressure measurement and consolidated in the triaxial cell under a backpressure of 200kPa to ensure full saturation and rapid pore pressure response. The average B value (Skempton, 1954) for all samples was 0.98, and any samples that did not have a B value of at least 0.96 were discarded. The stress state on the hollow cylinder sample is shown in Figure 1.

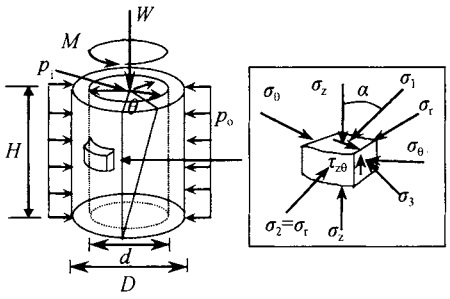

Figure 1. Stress state of soil element in hollow-cylinder soil sample

Test characteristics

To simulate the cyclic stress induced by wave loading which characterized by the fact that the orientation of principal stress axe rotates progressively, the phase different of the axial pressure and the torque are kept with 90° in the bi-directional cyclic loading tests. Figure 2 shows both the two cyclic components recorded in the test.

A total of 19 bi-directional cyclic loading tests will be discussed. Three various areas bounded by the elliptical stress path followed during the test in terms of $\sigma_d/2$ and τ are employed. And for each area the amplitude of the axial and shear stresses are kept changing to research the effect of each component on the strength and deformation behavior of saturated loose sand. To discuss the effect of each component on behavior of dynamic shear on sands, the specific value of the amplitude of dynamic axial stress and shear stress is defined as $(\sigma_d/2)/\tau=\lambda$. Furthermore, a radius $\sigma^*=\sqrt{(\sigma_d/2)\times\tau}$ of the circle whose

area is equal to the elliptical area is evaluated to study the effect of elliptical area on strength of sands in liquefaction. There are two methods to be applied in the tests.

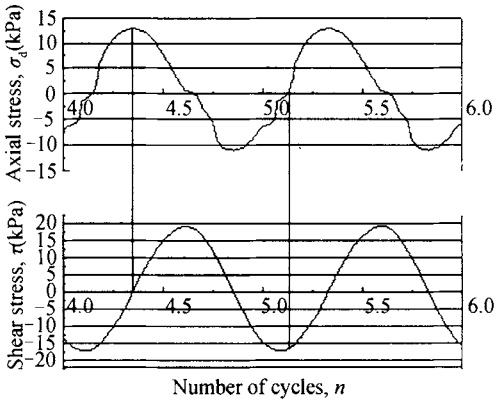

Figure 2. Cyclic components recorded in the test

(1) Several samples are subjected to cyclic loading following the elliptical stress path with constant ellipse area, but with λ varied. In this type of tests there are total three different ellipse areas employed, and at least four samples tested with different specific value λ for each ellipse area. When λ is much less than 1, the bi-directional shearing could be simplified to torsional shearing approximately. And when λ is much larger than 1, the bi-directional shearing could be simplified to triaxial shearing approximately. Figure 3 shows the loading patterns changing from similar cyclic triaxial shearing to similar cyclic torsional shearing.

The tests are investigated to simulate the decreasing ratio of vertical to horizontal accelerated speed occurring from near field earthquake to far field earthquake. The similar cyclic triaxial test is shown in Figure 3(a), in which the axial stress is much larger than shear stress as near field earthquake condition.

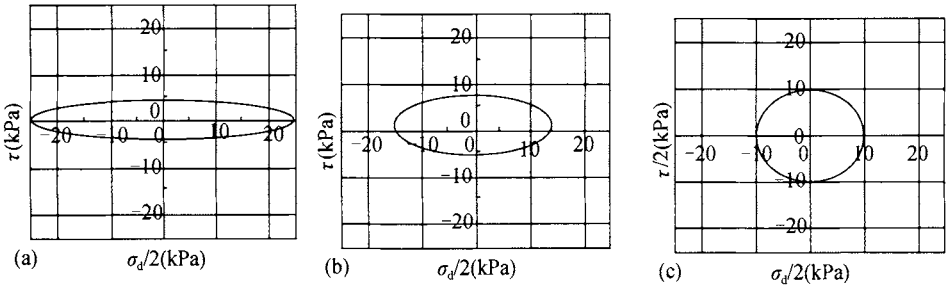

Figure 3. Stress paths in bi-directional cyclic shearing under isotropic consolidation

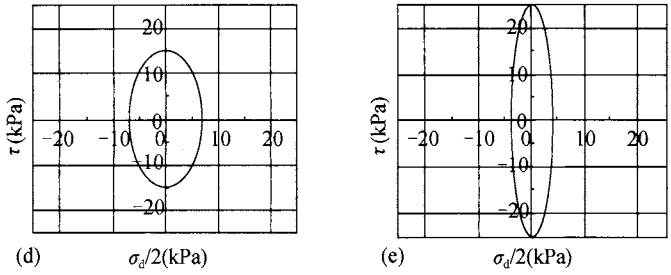

Figure 3. Stress paths in bi-directional cyclic shearing under isotropic consolidation (continued)

(2) Several samples are subjected to cyclic loading following the elliptical stress path with different ellipse area, but with λ constant. In this type of tests there are total five different values of λ employed, and at least two samples tested with different ellipse area for each λ.

The two actual stress paths recorded in tests shown in Figure 4 represent the specific value of λ larger and less than one respectively. It can be seen that the tests methods are valid, for which can realize the principal stress rotating progressively and the alteration of each cyclic component.

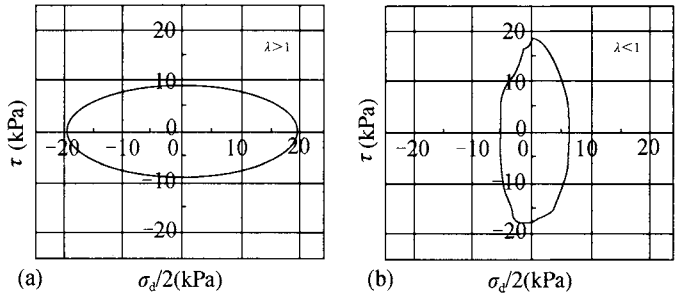

Figure 4. Stress paths recorded in vertical-torsional coupling shear tests under isotropic consolidations

TEST RESULTS AND DISCUSSION

Liquefaction

When a sand is subjected to cyclic shear loading under undrained conditions, the pore-water pressure rises, and consequently, the effective stresses decrease. If loading is continued, the pore water pressure may develop to the initial effective confining pressure and the effective stresses may be reduced to zero, resulting in what is known as liquefaction, as shown in Figure 5. Failure due to cyclic loading is defined by development of the pore-water pressure reaches its initial effective confining pressure.

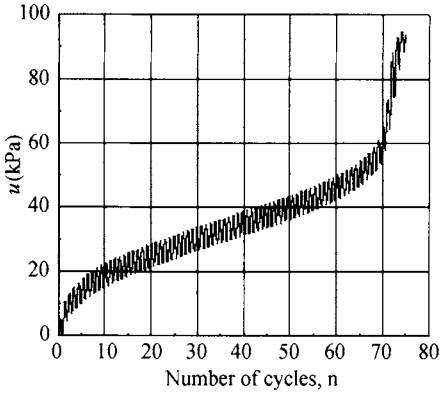

Figure 5. Pore pressure recorded in bi-directional cyclic loading

Strength

The liquefaction strength of saturated sand is commonly evaluated by undrained cyclic traixial test with two-way loading in compression and extension (Hyde 2006). That is because the laboratory testing equipment is not generally available for performing tests which model multidirectional loading conditions (Boulanger, 1995). This paper considered more complex stress conditions of bi-directional cyclic shearing than one-directional cyclic shearing such as cyclic traixial shearing. Thus bi-directional cyclic testing is capable of providing comprehensive conclusions in liquefaction. Using bi-directional cyclic loading tests the writers have therefore attempted to provide qualitative guidance on the effects of the two orthogonal cyclic components.

Figure 6 shows the relationships between λ and number of cycles to cause failure for each area of the elliptical stress path. Figure 7 shows the relationships between σ^* and number of cycles to cause failure for each identical λ.

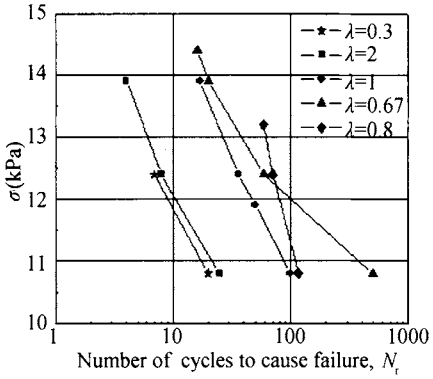

Figure 6. Relationship between λ and N_f

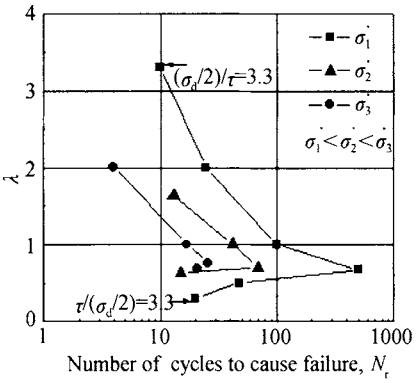

Figure 7. Relationship between σ^* and N_f

The tests results show that the strength of sand is closely associated with both the area of elliptical stress path and the ratio of two stress components λ. The specimen has a lower resistance to liquefaction if tested under elliptical stress path of a greater area. For the same area of elliptical stress path, sand behaves the highest cyclic loading resistance at a critical value of λ, which equals to 0.6~0.75. The cyclic loading resistance of sand increases with the decrease of λ when λ is larger than the critical value, whereas the resistance increases with the increase of λ when λ is less than the critical value. Moreover, for two types of stress combination with the same value of $(\sigma_d/2)/\tau$ and $\tau/(\sigma_d/2)$, the former one will result in the failure of sand more rapid, as shown in Figure 6. It shows that the cyclic loading resistance of saturated loose sand under similar cyclic torsional test is larger than that under similar cyclic triaxial test, which is uniformity with results of Guo (2003) and Boulanger (1995).

It can be clarified from Figure 7 that the cyclic resistance to liquefaction of sand decreases with the increase of ellipse area when λ is invariable. Moreover, the critical value of λ is increasing gradually with the ellipse area.

As a result, it should be comprehensively considered about in evaluating the cyclic resistance of sand to liquefaction, that both the area of elliptical stress path and the amplitude ratio of two orthogonal cyclic components.

Deformation

Figure 8, 9 (a), (b), (c) represent the undarined cyclic response of sand subjected to bi-directional cyclic loading with different λ but same ellipse area bounded by elliptical stress path. For isotropically consolidated samples, strain amplitude suddenly increased at an occasion and the sample failed within a few cycles. Such a rapid accumulation of strain, characteristic of loose sands, is now more commonly known as liquefaction failure.

The relationships between cyclic axial stress (σ_d) and axial strain (ε_v) are illustrated in Figure 8. Regarding to Figure 8 (a), (b), (c), sand exhibits softer behavior in extension side although the amplitude of cyclic stress is the same both in the compression and extension sides. Axial deformation in extension side is also considerably larger. In the first case of λ less than the critical value, the sample undergoes cumulative permanent axial strain on single extension side, as shown in Figure 8 (a). Conversely, in other cases of λ larger than the critical value, sample undergoes cyclic permanent axial strains both in the extension and the compression side, of which the extension side occurs more remarkable strain, as shown [Figure 8 (b), (c)].

It also can be seen from Figure 8 (a) that major axial strain occurs during the phase axial stress unloading for λ less than the critical value. And converse feature that major axial strain occurs during axial stress loading can be observed for the case of λ larger than the critical value, as shown in Figure 8 (b), (c).

The relationships between cyclic shear stress (τ) and shear strain (γ_θ) are illustrated in Figure 9. Almost all the shear strains exhibit double directional cyclic nature. For the first case of λ less than the critical value [Figure 9 (a)], the sample undergoes symmetric cyclic permanent shear strains. Conversely, for other cases of λ larger than the critical value [Figure. 9 (b), (c)], the sample undergoes asymmetric cyclic permanent shear strains.

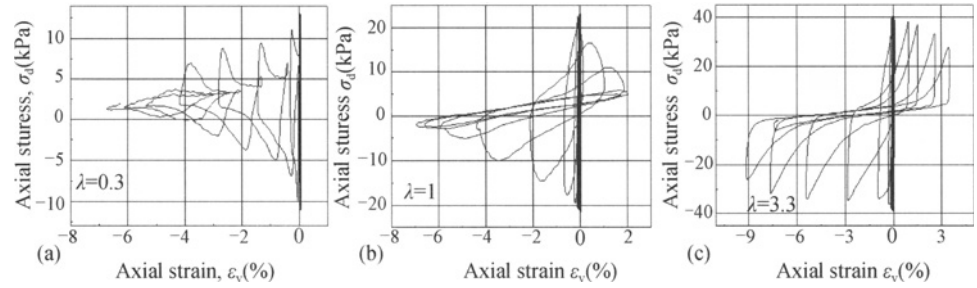

Figure 8. Relationships between axial stress and axial strain

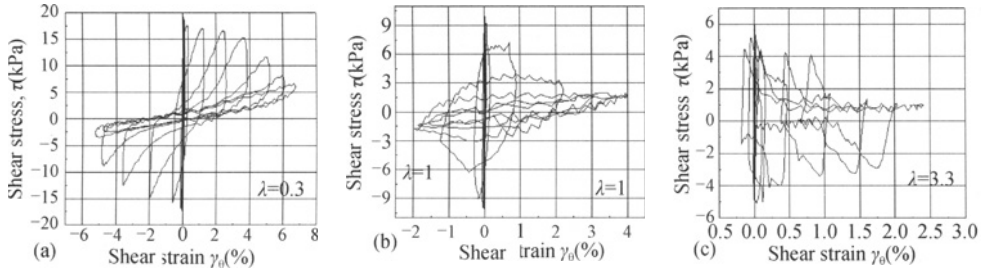

Figure 9. Relationships between shear stress and shear strain

Cyclic stress paths

Figure 10, 11 show typical effective cyclic stress paths corresponding to the cyclic stress-strain behaviors illustrated in Figure 8, 9. The rate of reduction in effective stress during cycling was approximately constant at the beginning of a test. However, as soon as the strain amplitude increased, the rate of reduction bacame increasing and the samples liquefied within 2-4cycles, characterized by transient excursions of the stress path through the origin (Ghionna and Porcino, 2006).

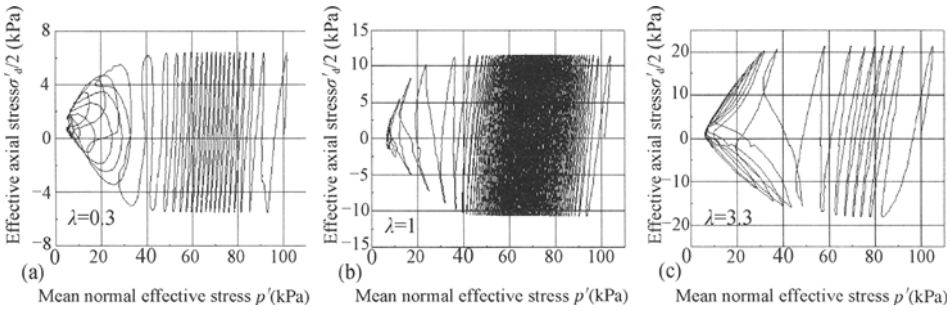

Figure 10. Relationships between effective axial stress and mean normal effective stress

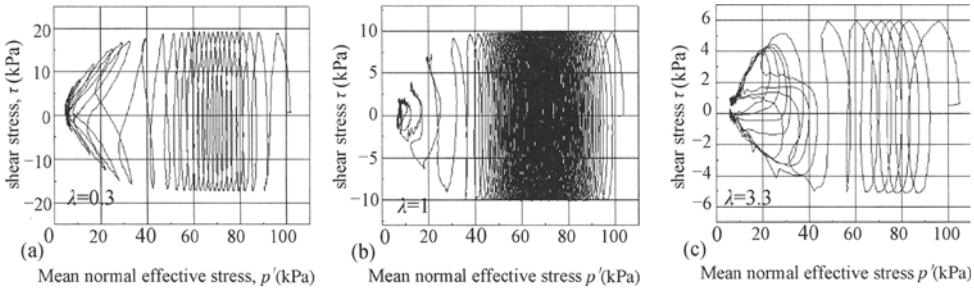

Figure 11. Relationships between shear stress and mean normal effective stress

Pore water pressure

Figure 5 depicts a trend with a number of cycles (N_f) cyclically induced pore water pressures (u). It can be observed that both the peak and valley values of u appear in one cycle, which means both dilative and contractive deformation occurs in the sample. But the extent of contraction is eventually greater than dilatation, which represented in the curve is that the residual pore water pressure develops gradually. Figure 12 (a), (b) illustrate $\sigma_d/2$, τ and u versus N_f curve. As marked in the figure, the pore water pressure and axial stress achieve their peak values at the same occasion in one cycle while the shear stress reaches the valley value.

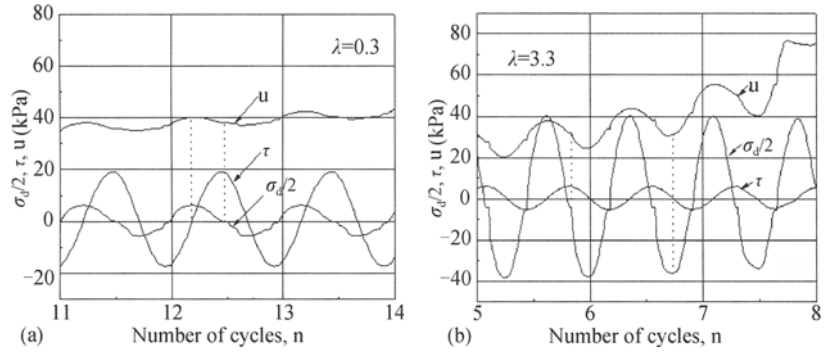

Figure 12. u, $\sigma_d/2$, τ –n curve

CONCLUSIONS

Undrained cyclic stress-strain-strength behavior of the Chinese Fujian Standard Sand has been investigated through cyclic bi-directional elliptical coupling shear tests. The main conclusions that can be drawn from the study may be summarized as follows:

(1) The cyclic resistance of sand is closely associated with both the area bounded by the elliptical stress path followed in terms of $\sigma_d/2$ and τ, and the ratio of $\sigma_d/2$ to τ. For the same λ, the resistance of sand decreases with the growth of ellipse area. There exists a critical value of λ. The sand may exhibit the highest resistance to liquefaction at this value for the same area of the elliptical stress path.

(2) When λ is less than the critical value, sample undergoes cumulative permanent axial strain only on the extension side and symmetric cyclic permanent shear strains on double direction.

(3) When λ is larger than the critical value, sample undergoes significant cyclic permanent axial strain both on the extension and the compression side, and much smaller asymmetric cyclic shear strains on double direction.

(4) The pore water pressure and axial stress achieve their peak values at the same occasion in one cycle while the shear stress reaches the valley value.

ACKNOWLEDGEMNETS

The authors wish to express their gratitude to Professor Dahong Qiu of Dalian University of Technology, who is a CAS's member, for his continuing support and invaluable advice for the investigation. The financial support for this study through the grant 50579006 and 50639010 from National Natural Science Foundation of China is mostly grateful.

REFERENCES

Boulanger R. W., Seed R. B. (1995). Liquefaction of sand under bi-directional monotonic and cyclic loading, *J. Geotech. Eng.*, 121 (12), 870-878.

Fu L., Wang H. J. and Zhou J. X. (2000). Effect of the initial rotation angle of principal stress on the dynamic properties of soil, *Chinese Journal of Geotechnical Engineering*, 22 (4): 435-440.

Ghionna V. N., Porcino D. (2006). Liquefaction resistance of undisturbed and reconstituted samples of a natural coarse sand from undrained cyclic triaxial tests, *J. Geotech. Geoenviron. Eng.*, ASCE, 132 (2): 194-202.

Hyde Adrian F. L., Higuchi T. and Yasuhara K. (2006). Liquefaction, cyclic mobility, and failure of silt, *J. Geotech. Geoenviron. Eng.*, ASCE, 132 (6): 716-735.

Luan M. T., Guo, Y., Li M. G., Wang J., Wang D. and Chong J. Z. (2003). Discussions on related key issues in development of soil static and dynamic universal triaxial and torsional shear apparatus, *Chinese Journal of Dalian University of Technology*, 43 (5): 670-675.

Pyke R. M., Seed H. B. and Chan, C. K. (1975). Settlement of sands under multidirectional shaking, *J. Geotech. Engrg. Div.*, ASCE, 101 (4): 370-398.

Seed H. B., Pyke R. M. and Martin G. R. (1975). Effect of multidirectional shaking on liquefaction of sands, Rep. No. EERC 75-41, University of California, Berkeley.

Skempton, A. W. (1954). The pore-pressure coefficients A and B, *Geotechnique*, 4 (4): 143-147.

Vaid, Y. P. and Chern, J. C. (1983). Effect of static shear on resistance to liquefaction, *Soils Found.*, 23 (1): 47-60.